Analysis of fretting fatigue failure

R. Kieselbach, R. Primas
Metallic and Ceramic Materials, EMPA-Dübendorf, CH-8600 Dübendorf, Switzerland

Abstract

The failure of a shaft after a relatively short service life has been analyzed. Based mainly on the fractographic investigation the failure was attributed to fretting fatigue. The fretting was caused by the contact of an inner ring of a roller bearing on the shaft. Material properties and in-service loads showed no significant deviations that could have led to the failure. A new design has been put in service to prevent future failure due to fretting fatigue. A numerical analysis by the finite element method was performed to compare the new to the old design with respect to fretting.

The local load situation in the contact area was modeled and the mechanical parameters most important for fretting fatigue were identified. For this purpose the zone of contact was specially treated using gap-friction elements in the finite element models.

The possibilities and limitations of a commercial finite element software for the analysis of a contact problem are shown. General rules for the improvement of shrink fit designs are derived.

According to the numerical analysis the improved design will be safe with respect to fretting fatigue in the contact area.

1 Introduction

The failed shaft was located at the summit station of a cable car and belonged to a system of wheels and shafts applying a pretension of 235 kN to the hauling and suspension cable. The cable was guided by two large wheels that were mounted on the failed shaft. One wheel was shrink fitted directly to the shaft while the other wheel was supported on roller bearings. The inner rings of the roller bearings were mounted onto the shaft. The old design is shown in Figure

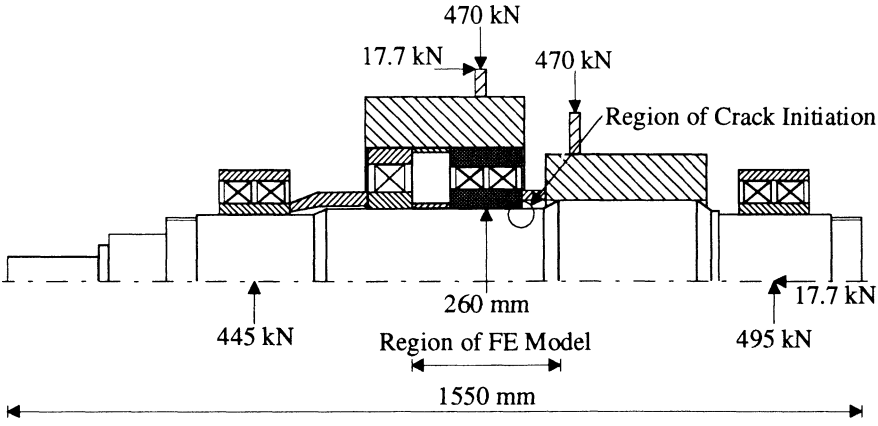

Figure 1: Schematic of the old shaft design

1. The fretting fatigue crack initiated in the shaft below an inner ring of a roller bearing. The inner diameter of the roller bearing measures 260 mm. The radial fit between the inner ring and the shaft ranges from -17.5 μm (interference) to +16 μm (inner ring oversized compared to the shaft). After only three years service the shaft showed considerable eccentricity and had to be replaced. The shaft was not broken completely. No accident or injuries had occurred.

A new shaft was installed in 1993 and its design is shown in Figure 2. The new design features a tension rod through the center of the shaft. It applies an axial compression force of 3 MN to the shaft. The inner diameter of the roller bearing under which the fretting fatigue crack initiated in the old shaft design has been increased to 360 mm. This enabled the contact area between the inner ring and the shaft to be removed from the main bending stresses in the shaft.

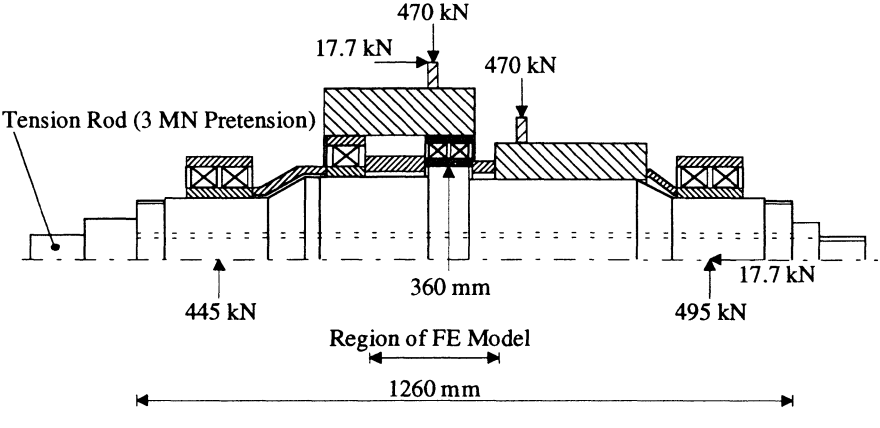

Figure 2: Schematic of new shaft design

The shrink fit has been changed to always ensure an interference. The radial interference ranges from -57 to -95 μm. The material of the shaft is in both cases 34CrNiMo6 (DIN material number 1.6582).

A failure investigation on the old shaft provided information on the cause of the failure. The goal of the numerical analysis was to qualitatively compare the old to the new shaft design regarding their susceptibility to fretting fatigue. The mechanical parameters most important for fretting fatigue are (e.g. Kreitner et. al. [1]):

- the amount of the local alternating slip between the inner ring and the shaft
- alternating shear stresses acting on the contact area (if local slip occurs the shear stresses depend on the local radial pressure in the shrink fit)
- local von Mises stresses in the shaft at the contact area (a stress concentration occurs due to a change in stiffness)

Finite element models were used to model the local load situation around the contact area. The above mentioned mechanical parameters were identified and used to judge the susceptibility of the old and new shaft design to fail due to fretting fatigue.

2 Failure Investigation

The failure analysis on the old shaft design included a visual inspection, fractography, metallography, and a tensile test. A standard stress analysis was performed to ensure that common engineering rules were not violated during the design phase.

The visual inspection revealed clear traces of fretting on the surface of the shaft under the inner ring of the roller bearing. A crack on the surface could be seen that extended approximately half around the circumference of the shaft in a slight angle with respect to the circumferential direction. When the shaft was cut and separated at the crack clear marks of a fatigue crack due to bending were revealed.

Fractography by scanning electron microscope and metallography showed that the fracture had started from a surface crack and that a multitude of similar surface cracks were present at the shaft surface. The angles between the small surface cracks and the shaft surface were small. The main fatigue crack leading to the failure had grown slowly and the area of the fatigue crack was nearly 60% of the whole cross section.

A tensile test of a specimen taken close from the fracture location resulted in a yield strength $R_{p0.2}$ = 686 MPa, ultimate strength R_m = 841 MPa, elongation after fracture ε_{A5} = 18%, and a reduction of area of 58.3%. All these values exceed the requirements stated in DIN 17200 for this steel.

The loads acting on the old shaft design are shown in Figure 1. These loads result in a nominal bending stress of 108 MPa at the cross section where the fretting fatigue crack occurred. If a fatigue strength of 385 MPa is taken and its reduction due to shape factor and stress concentration is considered, one gets

an allowable stress of 159 MPa. Therefore, a stress analysis following standard engineering rules (e.g. Decker [2]) does not reveal a potential for failure.

3 Numerical Analysis of the Contact Problem

The numerical analysis was performed to ensure that the new shaft design indeed improves the fretting fatigue behavior. For this purpose the regions around the critical contact areas of the old and new shaft design have been modeled with three-dimensional finite element models. The modeled regions include the inner ring of the roller bearing and part of the shaft. The distance sleeves were not modeled but partly replaced by axial springs. Figure 1 indicates the modeled region of the old shaft design and Figure 2 the region of the new shaft design. Due to symmetry only half of the two structures had to be modeled. Three-dimensional isoparametric elements with eight nodes per element and gap-friction elements were used. The gap-friction elements provide frictional and gapping connections between any two nodes of a structure. The finite element model of the new shaft design is shown in Figure 3.

In the commercial finite element program [3] used for the analysis the

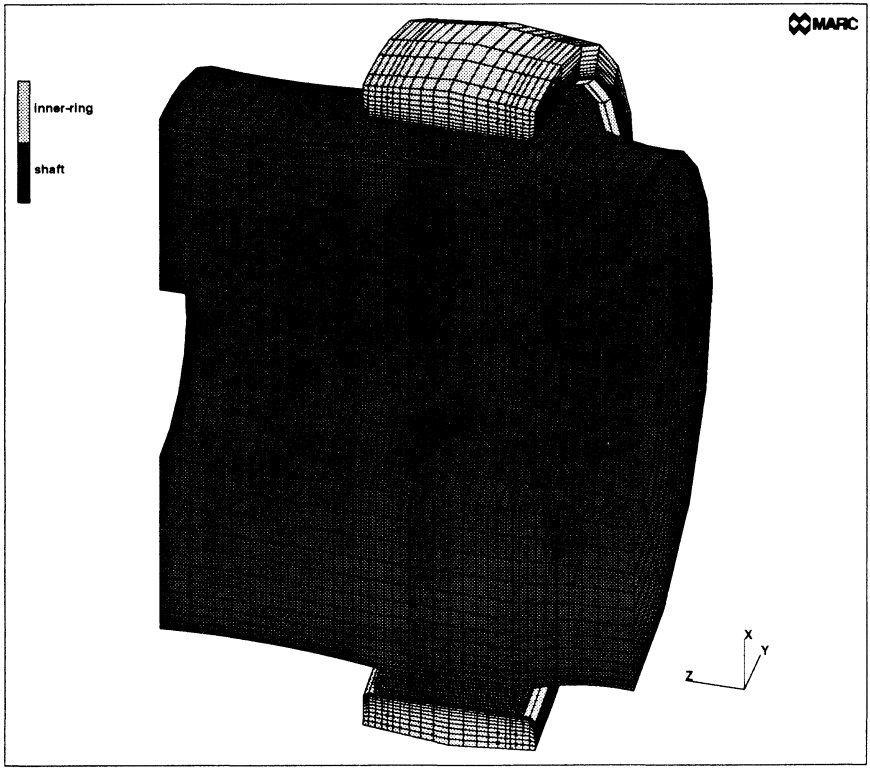

Figure 3: Finite element model of new shaft design

modeling of gap-friction is based on the imposition of kinematic constraints. The minimization of the total potential energy is subject to these constraints. This necessitates the introduction of Lagrange multipliers and the solution of an expanded system of equations. Conditional logic determines when to enforce a constraint or when to ignore it. During the evaluation of the stiffness matrix the gap status (open, frictional stick, or frictional slip) is based on the estimated strain increment. The gap status is checked again after the solution is obtained. For cases where the gap status differs between assembly and recovery due to penetration or change from slipping to sticking friction, reiteration is enforced. Once contact between two components has been established the question of frictional forces and possible slip arises. Two frictional constraints are activated upon contact. Two frictional directions are perpendicular to each other and form the plane normal to the direction in which contact is established. If the frictional force exceeds the maximum allowed, based on the normal force and the coefficient of friction, an additional slip constraint is necessary to limit the magnitude of the friction force [4].

The loads carried by the old and new shaft design are shown in Figure 1 and Figure 2, respectively. The pretension of the cable results in a radial force of 470 kN acting on the wheel. Some of this load is transmitted to the shaft through the critical roller bearing. A constant pressure has been applied to the outer diameter of the inner ring around the upper half of the circumference to account for the radial load in the finite element models. The axial load of 17.7 kN is due to the weight of the wheel and is applied with a constant pressure all around the outer diameter of the inner ring. The nominal bending stresses due to the radial forces, the nominal axial stress due to the weight of the wheel and, in the case of the new shaft design, the nominal axial compression stresses due to the pretension of 3 MN act at the two ends of the modeled shaft.

Coefficients of friction between 0.4 and 0.8 are given in the literature for shrink fits between two steel components, e.g. Kreitner et. al. [1] and Häusler [5]. The largest local slip can be expected for a small coefficient of friction. For the analysis a value of 0.4 has been assumed.

The material behavior has been modeled as linear elastic. Young's modulus $E = 210'000$ MPa and Poisson's ratio $\nu = 0.3$ were assumed.

4 Results and Discussion

The material properties of the failed shaft were within standard limits. The operating stresses calculated by following standard engineering practice were on the safe side. The main crack leading to the failure was clearly a fatigue crack. Along the edges of the contact area numerous smaller surface cracks were found. The position and appearance of the surface cracks indicated that they had been initiated due to fretting fatigue. Traces of fretting on the shaft surface confirm the fractographic and metallographic findings.

The numerical analysis of the contact problem indicates that in the case of the old shaft design the contact between shaft and inner ring is lost during operation on the opposite side of where the radial force acts. If the inner ring is

radially oversized by +16 μm the loss of contact occurs along the whole width of the roller bearing while for a radial interference of -17.5 μm the contact is only lost at the edges of the roller bearing over a width of approximately 20 mm on both sides. The complete loss of contact over part of the circumference for the oversized inner ring resulted in numerical problems because the system of equations becomes ill-conditioned. This reflects the true physical behavior. Chattering may occur during operation that is only limited by the distance sleeves on both sides of the roller bearing (see Figure 1). The numerical problems have been overcome by introducing axial springs replacing the effect of the sleeves.

The increased interference fit in the new shaft design improved the contact situation. The inner ring remains over the whole width and around the full circumference in contact with the shaft during operation.

The local alternating slip between the inner ring and the shaft is an important parameter influencing the fretting fatigue behavior. The larger the slip the more likely fretting fatigue will occur. Figure 4 shows the range of slip that occurs during one revolution of the shaft for the old shaft design with a radial interference of -17.5 μm and the new shaft design. The slip is practically identical for the whole possible interference range of the new shaft design. The maximum alternating slip reaches 61 μm in the old shaft design and occurs in Figure 1 at the right hand side of the roller bearing which corresponds to the location where the cracks initiated. The maximum alternating slip in the new shaft design is approximately 2 μm. The alternating slip is the difference between two approximate values. Therefore, the exact numbers stated here can not be completely trusted. However, the numerical study indicates a large difference between the old and new shaft design and a qualitative statement can still be made.

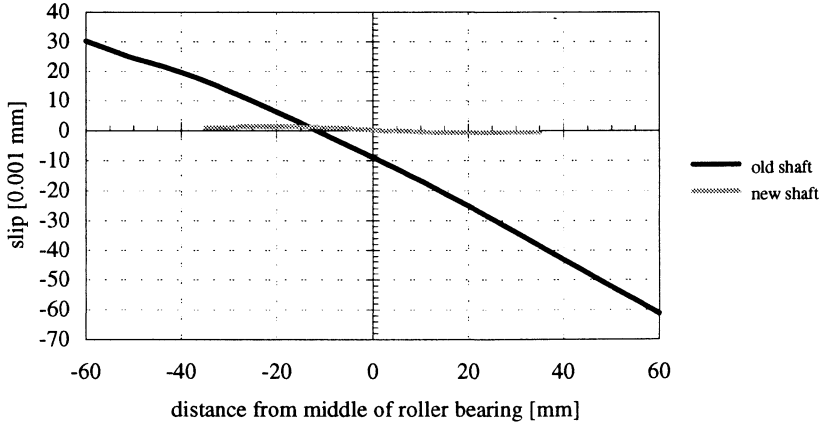

Figure 4: Range of local slip occurring during each revolution of the shaft for the old (radial interference: -17.5 μm) and new shaft design.

The used finite element meshes were not fine enough to get exact results on the peak radial contact stresses at the ends of the roller bearings. The models indicate that the peak radial stress in the new shaft design is 50 to 70% of the peak radial stress in the old shaft design. A similar decrease of the shear stresses acting on the contact area can be expected. The increased inner diameter of the roller bearing is the main contributor for this improvement.

The contact area in the old shaft design is directly exposed to the bending stresses. The inner ring acts as a stiffness increase at the locations where the contact remains established during operation. This causes a stress concentration of the bending stresses. The stress concentration occurs at the ends of the inner ring where the material is most susceptible to fretting fatigue due to the combined effect of alternating slip and shear stresses. The stress concentration will accelerate the crack growth of small surface cracks initiated by fretting fatigue. Again, the finite element mesh is not fine enough to give exact results of the peak axial stress component. However, an increase of the axial stress component is clearly predicted by the finite element results.

The situation is completely different for the new shaft design. The contact area is removed from the effect of the bending moment. In fact, no axial stress component can act at the ends of the inner ring because of the shaft shoulder. However, the shoulder introduces an additional stress concentration in the shaft. Proper attention has to be paid to this stress concentration.

5 Conclusions

The failure of the old shaft has been attributed to fretting fatigue. The combined effect of local alternating slip and shear stresses initiated several small surface cracks in the shaft close to the edge of the contact area. One of these cracks grew due to the stress concentration at the edge of the inner ring and later due to the global bending stresses. The global bending stresses were small and only caused slow crack growth. After three years the shaft had to be taken out of service because considerable eccentricity hindered the safe operation.

The numerical analysis of the old shaft design predicts large local slip at the location where the surface cracks initiated and a stress concentration that enabled the continued growth of the cracks. These results are consistent with the findings of the failure analysis.

The numerical analysis of the new shaft design predicts a considerably smaller slip, smaller shear stresses and the absence of an axial stress component at the critical locations. Accordingly it can be concluded that the new shaft design will be safe with respect to fretting fatigue in the contact area.

The numerical study shows that contact problems can be analyzed with a commercial finite element program using gap-friction elements. Local effects influence the fretting fatigue behavior. This necessitates detailed modeling and results in long CPU times to obtain the solution. The use of many gap-friction elements requires many iterations to obtain the state of equilibrium even for linear elastic material behavior. A comparative study can lead to satisfactory results if the differences between the two or more considered designs are large.

The following general rules for the improvement of a shrink fit design can be derived from the results of the investigation:

- The radial interference should be large enough to ensure complete contact of the two components during operation. This will decrease the local alternating slip. On the other hand, if complete contact during operation can be guaranteed, an additional increase of the radial interference will just increase the local stresses and will be detrimental to the fretting fatigue behavior.
- The edges of the contact zone should be isolated from the effects of global external loads. Otherwise additional stresses will accelerate the propagation of surface cracks initiated by fretting fatigue. An additional positive effect arises from the fact that in this case the deformation of the two contact partners are more likely to be equal or at least similar and, therefore, reduce local slip.

6 References

[1] L. Kreitner, H.W. Müller; *'Die Auswirkung der Reibdauerbeanspruchung auf die Dauerhaltbarkeit von Maschinenteilen';* Konstruktion 28 (1976); S. 209–216

[2] K.-H. Decker; *'Maschinenelemente';* Carl Hanser Verlag, München Wien; 1992

[3] MARC Version 5.2; MARC Analysis Research Corporation; Palo Alto, USA

[4] *'MARC User Information, Volume A';* MARC Analysis Research Corporation; Palo Alto, USA

[5] N. Häusler; *'Zum Mechanismus der Biegemomentübertragung in Schrumpfverbindungen';* Konstruktion 28 (1976); S. 103–108

7 Acknowledgement

The authors express their gratitude to the directors of EMPA for their support and permission for this publication.